CONTROL OF LOCOMOTION IN AMBULATORY AND AIRBORNE INSECTS USING IMPLANTED THERMAL MICROSTIMULATORS

Karthik Visvanathan[1], Naveen K. Gupta[1], Michel M. Maharbiz[2] and Yogesh B. Gianchandani[1]
[1]Department of Mechanical Engineering, University of Michigan, Ann Arbor, Michigan, USA
[2]Department of Electrical Engineering and Computer Science, University of California at Berkeley, USA

ABSTRACT

This paper describes the use of implanted microthermal stimulators for locomotion control of ambulatory and airborne insects. In the long term, this research is intended to support micro autonomous vehicles. Experiments were performed using both resistive (nickel), and piezoelectrically driven ultrasonic (PZT-5A) thermal stimulators on green june beetles (GJB) (*Cotinis nitida*) and Madagascar hissing roaches (*Gromphadorhina Portentosa*). Ultrasonic heating was 2x more power efficient, requiring 330-360 mW of input power to achieve the 43ºC pulses necessary for stimulation. Both stimulators demonstrated the feasibility of locomotion control with a success rate of 80% on GJB and 93.5% on the roaches. The microthermal stimulation resulted in average turn angles of 15-18º and 30-45º on GJB and roaches, respectively. Left and right turns were statistically similar.

KEYWORDS

Micro-vehicles, thermal stimulation, piezoelectric actuation

INTRODUCTION

Advances in communications and microfabrication capabilities have resulted in an increase in interest among researchers to investigate micro vehicles. Intended as mobile platforms for micro sensors and actuators, these may be used for military and civil applications [1-2]. In addition, the agility of airborne and ambulatory insects over wide ranges of mass and size has motivated research in controlling their locomotion for similar purposes [3] (Fig. 1). The optimized locomotion mechanism developed
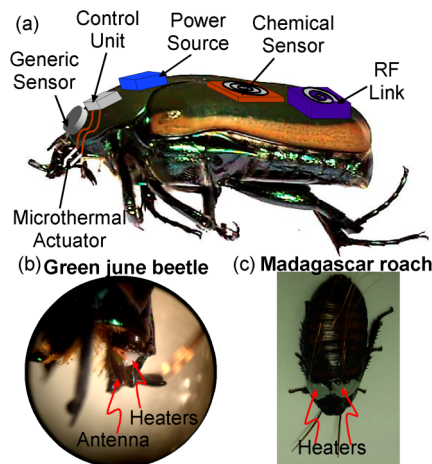

Fig. 1: (a) Concept of instrumented insect. (b) Enlarged side view of the head of the green june beetle with thermal stimulators near the antenna. (c) Photo of Madagascar hissing roach with implanted thermal stimulators

over thousands of years of evolution may provide superior payload capacity and travel range or reveal designs suitable for conventional approaches.

Past work in this vein includes preliminary efforts that used electroneural stimulation for beetles and roaches [4-6][7-8]. The role of antennae in the flight stability of hawk moths was reported by Sane in [9]. We recently reported on the feasibility of micro-thermal stimulation for steering beetles by bonding joule heaters near the antennae [10]. However, this early effort yielded a modest success rate (60%) and power efficiency.

In this paper, we compare the results of microthermal stimulation using joule heaters to the use of implanted ultrasonic heaters. Two types of insects are investigated: the green june beetle (GJB), *cotinis nitida*, and Madagascar hissing roach, *Gromphadorhina Portentosa*. Efficacy and efficiency are evaluated for both resistive and ultrasonic heaters. The following sections present the analytical model of temperature at insect heater interface, device design and fabrication, experimental results, and the relevant discussion and conclusions.

ANALYTICAL MODEL FOR INSECT-HEATER INTERFACE TEMPERATURE

An analytical model was developed for predicting the temperature at the insect heater interface. For the present analysis, both the insect body and epoxy surrounding the heaters are assumed to be semi-infinite media. The temperature variation within each medium is also neglected in order to reduce the complexity of the model. The properties of the materials used in the analytical model are listed in Table 1. The equilibrium temperature at the interface is given by [11]:

$$T_o = \frac{T_1\sqrt{\rho_1 c_1 k_1} + T_2\sqrt{\rho_2 c_2 k_2}}{\sqrt{\rho_1 c_1 k_1} + \sqrt{\rho_2 c_2 k_2}} \qquad (1)$$

where T_1, T_2 are the temperatures of the first and the second semi-infinite bodies; ρ_1, ρ_2 are the densities of the two bodies; c_1, c_2 are the specific heat capacities, and k_1, k_2 are the thermal conductivities. The subscripts '1' and '2'

Table 1: Temperature at interface between heater (covered with epoxy) and insect.

Property	Insect shell	Epoxy
Initial Temperature, T (K)	300	393
Density, ρ (Kg/m^3)	1496	870
Heat Capacity, c (J/Kg.K)	3700	1100
Thermal Conductivity, k (W/m/K)	1	0.25

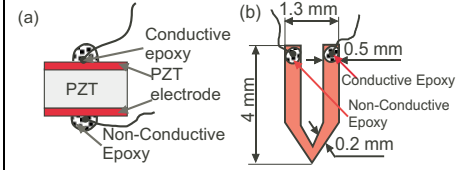| Table 2: Comparison chart for different types of stimulators used in the experiments on GJB and roaches.				
	Description	shape	Dim. (mm)	Property
R1	Joule heating	V	4x1.3x0.05	R= 2 Ω
P1	Piezo-thermal	O	Φ=3.2; h=0.2	C = 0.65 nF
P2	Piezo-thermal	▭	1x3x0.127	C = 0.37 nF
P3	Piezo-thermal	▭	1x0.5x0.127	C = 0.06 nF

Fig. 2: Thermal stimulators used. (a) Cross-section of P1/P2/P3. (b) Top view of R1.

denote the insect shell and epoxy (surrounding) the heater, respectively. Due to heat conduction in the surrounding tissue, the temperature at the interface of the heater and insect is lower than the bulk temperature of the heater. In our prior work, the interface temperature necessary for stimulation was estimated to be 43ºC. The model suggests that for reaching this interface temperature, the heater's core should be maintained at around 120ºC.

DEVICE DESIGN AND FABRICATION

Both resistive and ultrasonic heaters were designed and fabricated (Table 2, Fig. 2). While the resistive heaters work on the principle of joule heating, the ultrasonic heaters generate heat due to dielectric losses in the piezoceramics and damping losses in the surrounding medium. The piezoelectric ceramic PZT 5A was used for fabricating the ultrasonic heaters as it has a high Curie temperature (350ºC). Further, the piezoelectric constant and dielectric constant of PZT 5A show lower temperature dependence as compared to an alternate, PZT 5H.

The time constants of Ni and PZT stimulators were compared based on a simple analytical model. For a structure with convective boundary condition, scaled time constant (STC) can be defined as

$$STC = \frac{\tau A h}{V} = \rho\, c_p \qquad (2)$$

where τ is the time constant of the stimulator, A is the surface area of the stimulator, V is the volume of the stimulator, ρ is the density of the stimulator, c_p is the specific heat capacity and h is the convection coefficient of heat transfer. The STC aids in comparing the performance
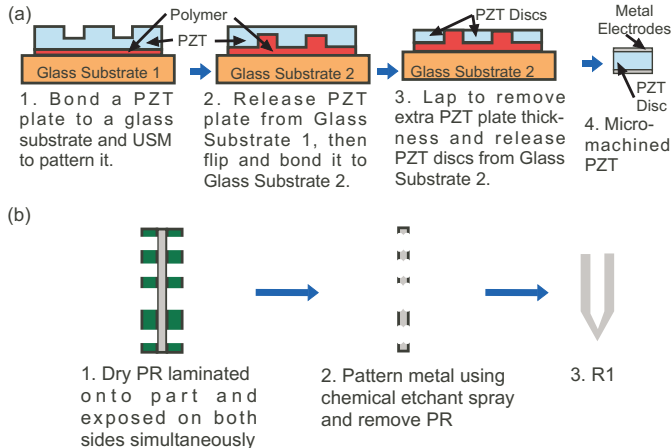
Fig. 3: (a) Ultrasonic machining for piezothermal stimulators. Fabrication of bulk Ni heater (R1) – metal foil is covered with dry photoresist, which is used to mask a spray etch.

of two stimulator materials irrespective of their geometry. This equation suggests that the STC of the piezothermal stimulators is about 55% of the bulk Ni stimulators. Further, the high impedance and low thermal conductivity of the PZT allows fabrication of thicker devices (that are easier to implant), as compared to resistive heaters, which need to be thin for higher efficiency.

The resistive heaters (R1) were fabricated from thin nickel foil (Fig. 3). Dry photoresist is laminated and patterned on both sides of the foil. The exposed metal is then spray etched (Fotofab Corporation, Chicago, Illinois, USA). An additional timed etch is performed to yield the thinned tip of the stimulator in order to concentrate the thermal energy. Finally the connecting copper wires (gauge ≈38, length ≈40 cm, resistance ≈0.2 Ω) are bonded to the stimulator using conductive epoxy, followed by a layer of non-conductive epoxy.

The circular piezothermal stimulators (P1) may be fabricated by ultrasonic machining (USM) of PZT 5A plate followed by metallization (Fig. 3)[12]. First, micro electro-discharge machining is used to fabricate the USM tool in stainless steel. Next, this pattern is transferred to a PZT 5A plate using USM with tungsten carbide slurry. Finally, the patterned PZT is released by lapping it from behind. A thin metal layer is deposited to serve as an electrode and provide the electrical contact. Circular PZT discs are also available commercially (Piezo Systems Inc., Woburn, Massachusetts, USA).

The rectangular PZTs (P2/P3) are fabricated by dicing a 127 micron thick PZT 5A plate into rectangular shape of 3x1 mm^2 and 1x0.5 mm^2, respectively. The electrical connections are provided by bonding copper wires using conductive epoxy followed by a layer of non-conductive epoxy for insulation.

EXPERIMENTAL RESULTS
Experiments on Green June beetle

The GJB response was quantified by restricting its movement using customized gimbal with an acrylic frame
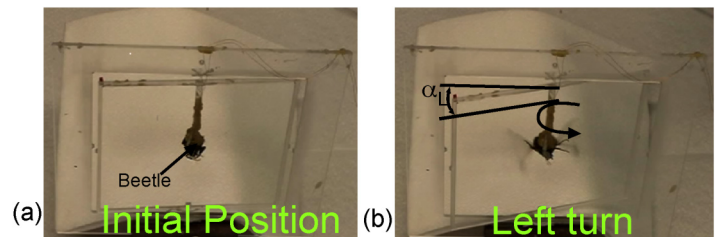
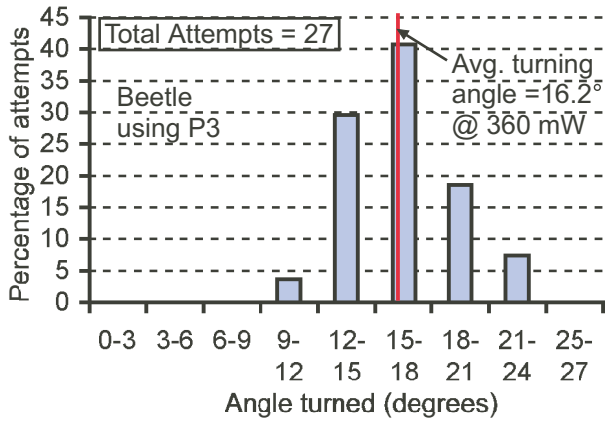*Fig. 4: Photo-graph of beetle turning towards left side due to actuation on right side*

Fig. 5: Turning characterization for P3 in GJB. P3 produces an average turning of 16.2° at 360 mW

Fig. 7: Turning characterization for P1 and P2 in roaches. Statistical variation of angle turned indicates that maximum count occurs in the range of 30-45 degrees at 330 mW.

and silicone flexures. The gimbal permitted rotational movement about its axis while restricting all the other degrees of freedom of movement. Its torsional stiffness was 67.8 mN-mm/rad. The beetle was attached to the gimbal using permanent magnets mounted on its back. The resistive and piezothermal stimulators were actuated using DC power supply (HP E3630A) and AC function generator (Agilent 33250A), respectively. For the resistive stimulators, both the voltage and the current through the stimulator were measured. The power consumed was given by the product of voltage across the stimulator and the current flowing through it. Similarly, the voltage and current across the piezothermal heaters were measured using an oscilloscope and Tektronix CT1 (1 GHz) current probe, respectively. The power dissipated by the PZT is given by:

$$P_c = V_{rms}I_{rms}\cos(\varphi) \qquad (3)$$

where φ is the phase difference between the current and the voltage, obtained by measuring the difference along the time axis between the maxima of voltage and the current signals.

In beetles the resistive and piezothermal stimulators were located near the antennae of the beetle on either side of the head: this region was empirically determined to be most sensitive to thermal stimuli. The enlarged view of the beetle head with implanted thermal stimulators is shown in Fig. 1b. Both resistive and piezothermal stimulators demonstrated the feasibility of flight initiation and direction control of GJB.

Piezothermal stimulators (P3) showed flight initiation and directional control of the GJB (Fig. 4) for an input power of 360 mW. The piezothermal stimulator P3 was actuated at its resonance frequency of 1.9 MHz because it attains maximum thermal efficiency around resonance. The beetles were stimulated about 34 times over a period of four days with an overall success rate of 80% thereby indicating the repeatability and replicability of the proposed technique. The beetles rotated away from side being heated by an average angle of 16.2°, which demanded a torque of about 19.2 mN-mm. Statistical results for repeated stimulation of P3 on beetle are shown in Fig. 5. In comparison, resistive stimulator R1 produced 15° turns at an input power of 800 mW.

Experiments on Madagascar roaches

The piezothermal stimulators P1 and P2 were used for
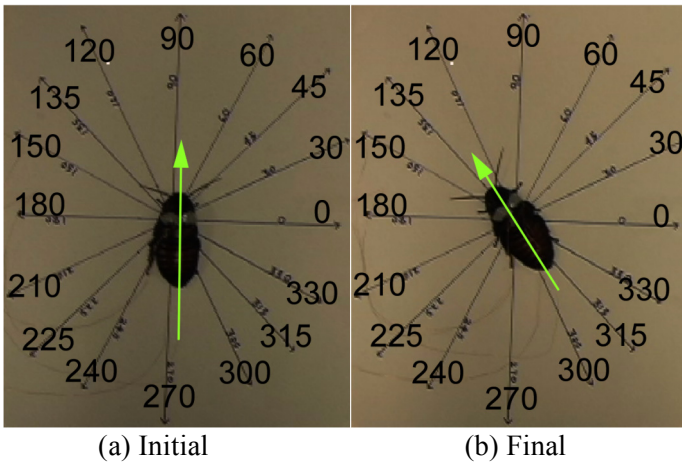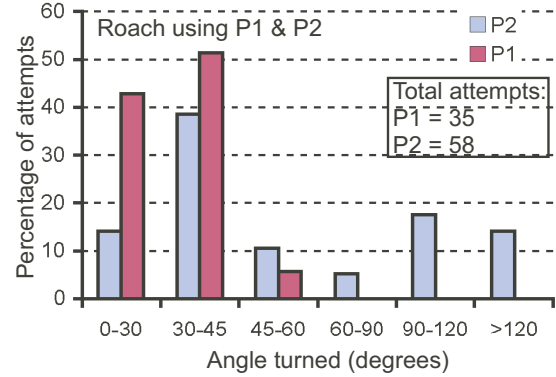

(a) Initial   (b) Final

Fig. 6: Photo-graph of the roach turning towards its left side due to the actuation of P2 on the right side. The angle turned was characterized by positioning the roach on the paper marked with angles
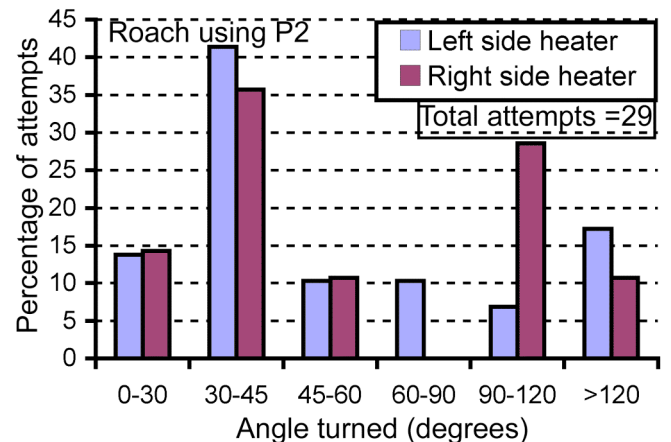

Fig 8: Left and right turning characteristics for P2 in roaches. The behavior was statistically symmetrical.

the experiments on the roaches. The stimulators were implanted on either side of the thorax near the head, as shown in Fig. 1c. In order to quantify the angle turned, the roaches were placed on a surface marked with angles as shown in Fig. 6.

The piezothermal stimulators were actuated as described in the previous section. Similar to the experiments on the beetles, both P1 and P2 were actuated around the resonance frequency of 4.2 and 5.5 MHz, respectively.

Like beetles, roaches turned away from the side being stimulated (Fig. 6). The stimulator P2 was more power efficient. It required 330 mW for actuation as compared to 550 mW for P1. Further, it showed superior directional control. About 93.5% of the total attempts were successful for P2 as opposed to 60% for P1. This is probably due to smaller size of P2, which resulted in localized heating.

The angle turned for repeated actuation of P1 and P2 was also measured. Figure 7 suggests that the roach on an average turn an angle of about 30-45º per actuation. As expected, the left and right turns were statistically similar as shown in Fig. 8.

CONCLUSIONS

This paper suggests the repeatability and replicability of implanted microthermal stimulation for locomotion control of both airborne and ambulatory insects. Piezothermal stimulators proved to be a better choice for the current application due to higher thermal efficiency. The smaller piezothermal stimulators were found to offer superior direction control. The thermal stimulation produced an average turn angle of 16.2º on GJB and 30-45º on roaches. The implanted microthermal stimulation resulted in a high success rate of 93.5% on roaches and 80% on beetles, while reducing the power consumption by half. Further, the proposed technique is generic in nature as compared to other techniques that depend on specific neurological or physiological structures.

ACKNOWLEDGEMENTS

REFERENCES

[1] S. Ashley, "Palm-size spy planes," *ASME Journal of Mechanical Engineering*, vol. 120, pp. 74-78, 1998.

[2] W. Shyy, P. Ifju, and D. Viieru, "Membrane wing-based micro air vehicles," *Applied Mechanics Reviews,* vol. 58, pp. 283-301, 2005.

[3] A. Paul, A. Bozkurt, J. Ewer, B. Blossey, and A. Lal, "Surgically implanted micro-platforms in manduca sextamoth," *Solid-State Sensor & Actuator Workshop*, Hilton Head, SC, 2006, pp. 209– 211

[4] K. Hausen, and C. Wehrhahn, "Neural circuits mediating visual flight control in flies. I. Quantitative comparison of neural and behavioural response characteristics," *Journal of Neuroscience*, vol. 9, pp. 3828-2836, 1989.

[5] H. Sato, C.W. Berry, B.E. Casey, G. Lavella, Y. Yao, J.M. VandenBrooks, and M.M. Maharbiz, "A cyborg beetle: insect flight control through an implantable tetherless microsystem," *IEEE MEMS*, Tucson, USA, 2008, pp. 164-167

[6] H. Sato, C.W. Berry, and M.M. Maharbiz, "Flight control of 10 gram insects by implanted neural stimulators," *Solid-State Sensor & Actuator Workshop*, Hilton Head, SC, 2008, pp. 90-91.

[7] S.B. Crary, T.E. Moore, T.A. Conklin, F. Sukardi, and D.E. Koditschek, "Insect biobotics: Electro-neural control of cockroach walking," *IEEE Robotics and Automation workshop WT3, Bio-Mechatronics*, 1996, pp. 42–54.

[8] S. Takeuchi, and I. Shimoyama, "An RF- telemetry system with shape memory alloy microelectrodes for neural recording of freely moving insects," *IEEE Special Topic Conference on Microtechnology in Medicine and Biology*, 2000, pp. 491-496,

[9] S.P. Sane, A. Dieudonne, M.A. Willis, T.L. Daniel, "Antennal mechanosensors mediate flight control in moths," *Science*, vol. 315, pp. 863-866, 2007.

[10] K. Visvanathan, N.K. Gupta, M.M. Maharbiz, and Y.B. Gianchandani, "Flight initiation and directional control of beetles by microthermal stimulation," *Solid-State Sensors, Actuators and Microsystems Workshop*, Hilton Head, SC, 2008, pp. 126-129.

[11] Y.A. Cengel, "Heat Transfer – A Practical Approach," *McGraw Hill*, pp. 244-271, 1997.

[12] T. Li, and Y.B. Gianchandani, "A micromachining process for die- scale pattern transfer in ceramics and its application to bulk piezoelectric actuators," *Journal of Microelectromechanical Systems*, vol. 15, pp. 605-612, 2006

CONTACT

Karthik Visvanathan, vkarthik@umich.edu
Yogesh B. Gianchandani, yogesh@umich.edu